Eur Biophys J (2010) 39:815–824
DOI 10.1007/s00249-009-0563-5

ORIGINAL PAPER

Phase transition kinetics of lipid bilayer membranes studied by time-resolved pressure perturbation calorimetry

Martin Schiewek · Alfred Blume

Received: 30 July 2009 / Revised: 23 October 2009 / Accepted: 30 October 2009 / Published online: 17 November 2009

Abstract The relaxation kinetics of aqueous lipid dispersions after a pressure jump (p-jump) was investigated using time-resolved pressure perturbation calorimetry (PPC). Analysis of the calorimetric response curves by deconvolution with the instrumental response function gives information about slow processes connected with the lipid phase transition. The lipid transition from the gel to the liquid-crystalline state was found to be a multi-step process with relaxation constants in the seconds range resolvable by time-resolved PPC and faster processes with relaxation times shorter than ca. 5 s that could not be resolved by the instrument. The faster processes comprise ca. 50% of the total heat uptake at the transition midpoint. This is the first calorimetric measurement showing the multi-step nature of the transition. The results are in good agreement with data obtained with other detection methods and with molecular modelling experiments describing the transition as a multi-step process with nucleation and growth steps.

Keywords Pressure jump · Phase transition · Phospholipids · Calorimetry · Kinetics

Abbreviations

DEPC	1,2-Dielaidoyl-*sn*-glycero-3-phosphocholine
DMPA	1,2-Dimyristoyl-*sn*-glycero-3-phosphatidic acid
DMPC	1,2-Dimyristoyl-*sn*-glycero-3-phosphocholine
DMPE	1,2-Dimyristoyl-*sn*-glycero-3-phosphoethanolamine
DOPE	1,2-Dioleoyl-*sn*-glycero-3-phosphoethanolamine
DPPC	1,2-Dipalmitoyl-*sn*-glycero-3-phosphocholine
DSPC	1,2-Distearoyl-*sn*-glycero-3-phosphocholine
PPC	Pressure perturbation calorimetry
SANS	Small-angle neutron scattering
T_M	Main transition temperature

M. Schiewek · A. Blume (✉)
Faculty of Chemistry and Physics, Institute of Chemistry,
Martin-Luther-University Halle-Wittenberg,
Muehlpforte 1, 06108 Halle (Saale), Germany
e-mail: alfred.blume@chemie.uni-halle.de

Introduction

Phospholipids dispersed in water show a complex lyotropic phase behavior displaying lamellar, hexagonal, and cubic phases. Transitions between different phases can be induced by changing the concentration, temperature, pressure or pH. Study of the kinetics of these phase transitions usually requires the application of techniques such as stopped-flow or relaxation methods where relaxation to equilibrium follows a fast change of an external condition (Eigen 1968). To study the kinetics of lipid phase transitions the pressure jump (p-jump) and temperature jump (T-jump) techniques are suitable methods for investigating the so-called main or chain-melting transition of lipid systems in which the transition occurs between the lamellar "gel" phase and the liquid-crystalline L_α-phase. This main transition is highly cooperative and occurs in multilamellar lipid samples over a very narrow temperature range. Because of the higher partial molar volume of the lipids in the liquid-crystalline phase it is also very pressure sensitive. The main transition shifts by about 22–25 K/kbar pressure increase for the most studied phospholipid dipalmitoyl-phosphatidylcholine (Liu and Kay 1977; Winter and Czeslik 2000; Kusube et al. 2005; Boehm et al. 2007). The pressure jump technique has certain advantages, because pressure jumps can be easily performed in both

directions and with various amplitudes. The time needed for a pressure jump can be as short as 10^{-5} s and the observation times can cover ranges from microseconds to hundreds of seconds. In contrast, temperature jumps can be performed much faster and the time resolution is therefore better. However, the total observation time is limited because of relatively rapid cooling processes after the jump. This makes T-jump experiments unsuitable for long time-scale experiments, where slow relaxation processes are to be expected.

Results of p-jump and T-jump investigations on aqueous lipid dispersions have already been reported—p-jump with turbidity detection (Gruenewald et al. 1980; Elamrani and Blume 1983; Blume and Hillmann 1986), T-jump with fluorescence probes (Gruenewald 1982; Genz and Holzwarth 1986), p-jump with X-ray scattering (Erbes et al. 2000) or FT-IR detection (Schiewek and Blume 2009), and, finally, pressure perturbation calorimetry (Grabitz et al. 2002; Boehm et al. 2007) have been used.

Interpretation of the results obtained has led to different concepts about the processes occurring during the transition. The turbidity and fluorescence measurements and the recently published p-jump experiments with FT-IR detection (Schiewek et al. 2007; Schiewek and Blume 2009) showed that the phase transition is a multiple step process with relaxation constants in different time regimes. The results were discussed in terms of nucleation and domain growth steps, similar to the cluster model of Kanehisa and Tsong (1978). It was assumed that the formation of domains of the new phase is the rate-determining step. As a consequence the transition is drastically slowed down at the phase transition midpoint temperature.

Other results have been obtained by use of methods sensitive to macroscopic properties only. Erbes et al. (2000) monitored changes of X-ray and SANS patterns after p-jumps. This technique is sensitive to the cooperative formation of clusters of the new phase and the development of ordered lamellar stacks of bilayers with defined thickness. These authors found that in some cases a third unknown state between the gel and the liquid-crystalline state occurred. This was observed for transitions of DEPC, for instance. This temporary phase could be monitored only after a rapid decay (<5 ms) of the pattern of the initial phase and could not be found among the thermodynamically stable phases in the p,T-diagram of DEPC. The authors describe indications of similar occurrences of intermediate states for the main transition of DOPE. They concluded that in most cases the phase transition kinetic is determined mainly by the transport and reallocation of solvent water, which is usually slow. Nucleation processes determine the kinetics only in those cases where the transition is much faster. In these cases water reallocation has little effect on the kinetics.

Pressure perturbation calorimetry is a method in which the heat flow between an aqueous lipid sample and the surroundings is monitored after a pressure jump or a periodic pressure perturbation. This method inherently has low time resolution, because the response time of the calorimetric instruments is in the range of seconds. Based on the results of p-jump calorimetry, a different concept for description of the transition was developed by Grabitz et al. (2002). The sample is described by an ensemble of highly cooperative sub-systems whose enthalpy is fluctuating because of energy exchange among the systems. When the ensemble is sufficiently close to the transition, a number of systems is already in the opposite phase. By use of the fluctuation–dissipation theorem it was shown that the fluctuation time (expressed by the decay constant of the enthalpy correlation function) is long near the transition midpoint. A suddenly induced transition cannot be faster than the time specified by the fluctuation time. This theory based on thermodynamics implies that the transition occurs as a *single* process. Furthermore the authors showed that proportionality should exist between the relaxation time τ and the heat capacity c_p. The relaxation rate was simulated on the basis of a two-dimensional Ising model to check this proportionality for validity. The τ–c_p-dependence was also studied experimentally by time-resolved calorimetric measurements. The authors (Grabitz et al. 2002) introduced pressure-resistant capillaries with the enclosed lipid sample into the calorimeter cell and could therefore reach pressures up to 40 bar. On the basis of their theory Grabitz et al. (2002) used a monoexponential function for regression analysis of the kinetic data. The monoexponential function had been convolved analytically with the instrument response function that describes the heat flow in the instrument. Similar calorimetric experiments were recently reported by Boehm et al. (2007). In these experiments, however, the pressure was applied directly to the sample cell of the instrument and the pressure was modulated ($\Delta p \approx 3$ bar) on a time scale shorter than the instrumental response time while heating the sample very slowly across the transition region.

The objective of the work discussed this paper was to elucidate the contradictory results of p-jump experiments using different detection techniques and the differences between the multi and single process concepts. We used time-resolved pressure perturbation calorimetry to check if multiple processes can be found in general and whether these are present only in the second time scale accessible by PPC only or also on shorter time scales. The experimental setup resembles that used by Boehm et al. (2007) but the data processing and analysis are different. We used a numerical procedure for deconvolution of the data instead of analytical convolution of the transition model. Our model-free approach was used to evaluate the number of

processes that are involved in the phase transition of aqueous phospholipid dispersions on time scales >10 s. However, we also detected the presence of processes connected with heat uptake that cannot be resolved by pressure perturbation calorimetry. Our results therefore support previous findings suggesting a multi-step mechanism of the phase transition of lipid lamellar phases.

Theory

The gel–fluid phase transition is accompanied by a volume change of 3–5%. Therefore the transition temperature shifts by approximately 0.09 K to higher temperature when the pressure is increased to 4.4 bar (cf. Fig. 1, top). The degree of transition θ can be calculated from the integrated and baseline corrected calorigrams using Eq. 1 where Δh_{total} corresponds to the total change in enthalpy or the area under the peak in the calorigram and $\Delta h(T)$ is the fractional change in enthalpy as a function of temperature T:

$$\theta = \frac{\Delta h_{\text{total}} - \Delta h(T)}{\Delta h_{\text{total}}} \quad (1)$$

with this definition, $\theta = 1$ for the gel phase and $\theta = 0$ for the liquid-crystalline phase. In a time-resolved p-jump experiment the pressure changes from excess to ambient pressure, which leads to a change of θ as indicated by the blue arrow in Fig. 1, bottom. In the experiment the change of θ can be measured as heat uptake. The transition should be slowed down strongly (longest relaxation time) if the end point is at the transition midpoint at ambient pressure, i.e. at $\theta = 0.5$ (cf. blue arrow and τ–T-function (black line) in Fig. 1, bottom). This is well-known from theory and previous experiments (Kanehisa and Tsong 1978; Gruenewald et al. 1980; Schiewek and Blume 2009). The maximum of the $\Delta\theta$ curve corresponding to the maximum amplitude (dashed blue curve), which is calculated from the difference between the two θ–T curves is always found at higher temperature compared with the maximum of the relaxation time τ. However, because of the low pressure changes of only 4.4 bar in the PPC experiment the transition temperature shifts by only 0.09 K and, therefore, the maxima in the τ–T and the θ–T curves appear at almost the same temperature within experimental error.

Experimental

Preparation of lipid suspensions

All lipids were purchased from Genzyme Pharmaceuticals (Cambridge, USA) and used without further purification.

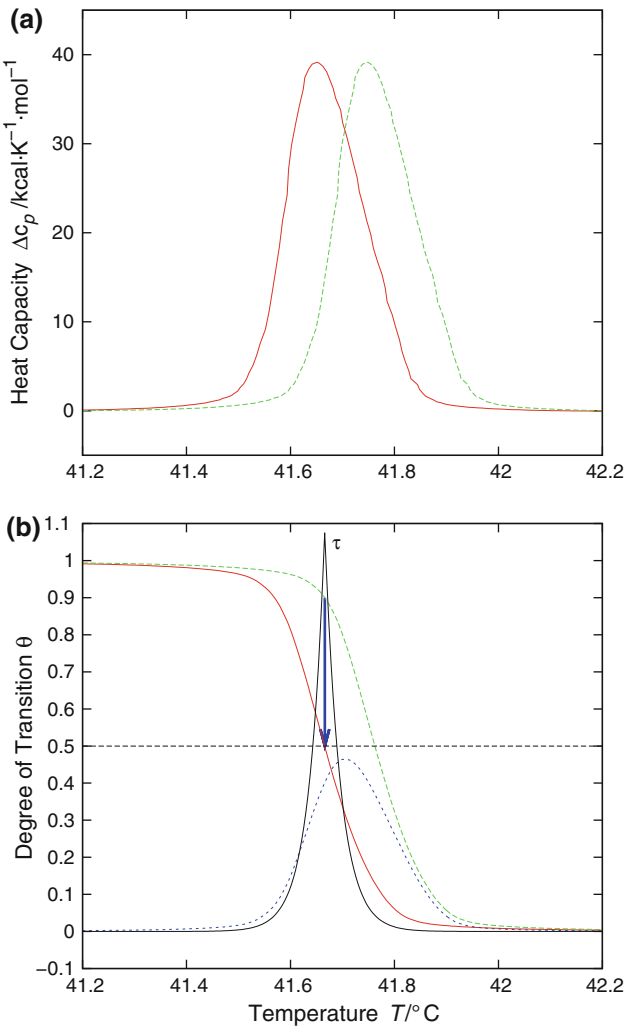

Fig. 1 *Top*: DSC trace of multilamellar vesicles of DPPC measured at ambient pressure (*red, solid*) using a heating rate of 1.5 K/h to minimize peak broadening because of the response time of the DSC instrument. Also shown is the calculated (*shifted*) curve, which would be measured at 4.4 bar excess pressure (*green, dashed*). *Bottom*: θ–T curves calculated from the data shown in the upper plot (*red*: *curve* at 1 bar, *dashed green*: *curve* with 4.4 bar excess pressure). The difference $\Delta\theta$ (*blue, dotted*) represents the amplitude as it would be appear in a p-jump experiment using isothermal conditions. The *blue arrow* stands for the amplitude when the slowest relaxation time is expected. The maximum of the τ–T curve (*solid black*, schematic representation, no ordinate values) is always found at lower temperatures compared to the maximum of the $\Delta\theta$ curve

All samples were prepared as multilamellar vesicles (50 mM) in ultrapure H_2O. The sample was heated to 10°C above the transition temperature T_M, vortex mixed and mildly sonicated until the sample was homogeneous. The sample was degassed under slight vacuum and then placed in the sample cell of the DSC instrument. The reference cell was filled with degassed water. Normal DSC experiments were used to check for the correct transition temperature T_M of the lipid dispersion.

Samples were not extruded to produce unilamellar vesicles because the long-term stability of these aggregates cannot be assured, due to the mechanical stress which is applied to the sample with each pressure jump and the long data acquisition times inside the transition region, which lead to fusion of unilamellar vesicles. In addition, the cooperativity of the transition of multilamellar vesicles is higher than that of unilamellar vesicles, which facilitates data analysis (Gruenewald et al. 1980).

Pressure perturbation calorimetry experiments

Time-resolved pressure perturbation calorimetry experiments were performed using a VP-DSC instrument equipped with a pressure-perturbation accessory (MicroCal, Northampton, MA, USA). This device is able to perform p-jumps from 4.8 bar (70 psi) excess pressure to ambient pressure or vice versa (Lin et al. 2002). Once the temperature was adjusted, the instrument was left to equilibrate for 5 min. After the measurement of a 30 s pretrigger interval, the evolution of the power signal was monitored for a maximum value of 999 s after the p-jump. During the experiment, the filter constant was set to 1 s and the response was set to "high" to achieve the best time resolution (Plotnikov et al. 1997).

Deconvolution of the kinetic PPC-traces

The shape of the measured signal $P_{\text{experimental}}$ can be described as the heat-flow signal P_{lipid} (generated by the lipid in the sample) convolved with the heat-flow response function R_{instr} of the instrument:

$$P_{\text{experimental}} = P_{\text{lipid}} \otimes R_{\text{instr}} \tag{2}$$

where "$\otimes$" denotes the convolution operator. Therefore, the pure lipid response P_{lipid} can be calculated by deconvolution of $P_{\text{experimental}}$ with the response function R_{instr}. The latter is unknown in the beginning, but can be determined if the signal from the sample behaves like a δ-function, because the convolution of a δ-function with the instrumental response function gives, again, the instrumental response function. A valid approximation to a δ-function is achieved if the heat release of the sample occurs immediately within the time of the pressure jump. To obtain the response function we measured $P_{\text{experimental}}$ using a solution of a small amount of ethanol in water versus pure water in the reference cell. The heat signal obtained in this type of PPC experiment is caused by the different thermal expansion coefficients of the solutions in the sample and the reference cell (Lin et al. 2002). The process of thermal expansion is very fast and thus fulfils the requirements for obtaining the instrumental response function by deconvolution.

The response function (cf. $\times$ symbols in Fig. 2) obtained by assuming a δ-function for the thermal expansion can be described by a biexponential function:

$$R_{\text{instr}} = \frac{k_1 k_2}{k_2 - k_1}[\exp(-k_1 t) - \exp(k_2 t)] \tag{3}$$

The time constants $\tau_i = 1/k_i$ were determined by regression analysis and were found to be temperature dependent (at 5°C: $\tau_1 = 1.6$ s, $\tau_2 = 6.3$ s; at 65°C: $\tau_1 = 2.7$ s, $\tau_2 = 5.5$ s). The measurements were carried out at several temperatures from 5 to 65°C. The temperature dependence of the time constants was then described using a polynomial function. The validity of the response function was checked by deconvolution of the ethanol–water response data, which should lead to a δ-like peak function. This test was performed twice: first using τ_i-values determined directly by the fit (cf. Fig. 2,open square symbols) and, second, with τ_i-values that were increased by 5% (asterisk symbols) to check for the influence of errors in τ_i on the deconvolved data. Both curves show much more δ-like behavior than the experimental curve, but still display an exponential decay (or increase) in the 2–10 s range, however with small amplitude. This is because Eq. 3 is merely a phenomenological description of the response function. Furthermore, the time constants τ_i determined from the regression analysis have a limited accuracy. In any case, the artifact amplitudes disappear at values $t > 10$ s, so that the deconvolution procedure offers the possibility of analysing time constants with values $\geq$10 s. Without deconvolution, only time constants with values >30 s could be determined. Hence, the deconvolution procedure improves

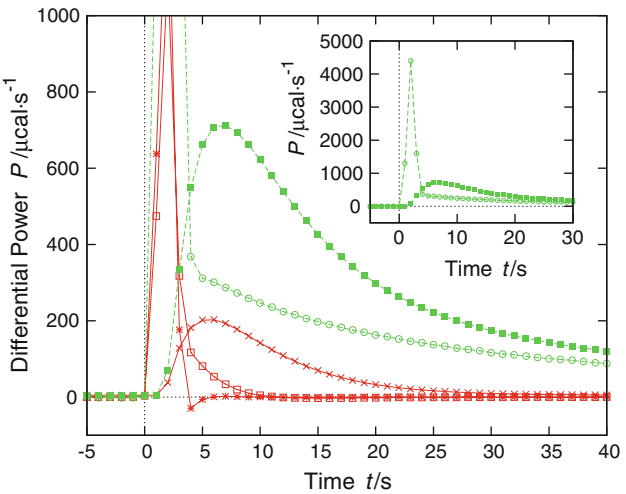

Fig. 2 *Red solid lines*, PPC response data for water with a small amount of ethanol: *multiplication signs*, raw data; *open squares* and *asterisks*, deconvolved data using slightly different τ_i-values according to Eq. 3. *Green dashed lines*, DSPC PPC-traces: *filled squares*, raw data; *open circles*, deconvolved data. The *inset* shows a full range view of the DSPC traces. See text for a detailed description

the time resolution by a factor of three. Figure 2 also shows, as an example, a curve from a series of temperature dependent traces of DSPC. While the experimental raw data (solid square symbols) are dominated by the instrumental response function, the deconvolved data (open circles) show clear separation of the instrumental response function from an additional exponential decay that starts 5 s after the jump. At times $t > 10$ s, this decay appears to be totally unaffected by the instrumental response and can therefore be used for the regression analysis and determination of the relaxation times of the transition kinetics.

The deconvolution algorithm was implemented using the Delphi7 programming language (Borland Software, Cupertino, USA). It includes FFT-algorithms for deconvolution from the book "Numerical Recipes" (Press et al. 1989).

Fitting of kinetic data

After the deconvolution the P–t-traces were fitted using a multiexponential model:

$$P(t) = \Delta P_{\text{base}} + \sum_{i=1}^{j} \Delta P_i \cdot \exp\left(\frac{t - t_0}{\tau_i}\right) \quad (4)$$

The baseline was described with a constant term ΔP_{base} to a first approximation. However, in the quasi-isothermal mode of the DSC instrument the temperature changes slightly with a rate of 10^{-5} K/s. This leads to baseline deviations at temperatures close to T_{M} caused by large changes of c_p. This is evident upon inspection of Fig. 3a, where the signal first decreases, because of relaxation processes, but then slowly increases again at longer times $t > 300$ s. Therefore, the number of points used for the regression analysis was limited to the range 10–300 s. For minimization of the error sum of squares χ^2 the simplex algorithm of Nelder and Mead was used (Nelder and Mead 1965; Press et al. 1989). It was implemented in the same program performing the deconvolution of the PPC traces. The number of exponential terms j was fixed to $j = 2$. Boundary conditions were used to keep all τ_i distinguishable and sorted in increasing order. A higher number of exponential terms would lead to lower values of χ^2 but the physical background of the time constants is questionable if they differ by less than a factor of five. Therefore, small systematic deviations in the residuals were acceptable, because the residuals and the noise level of the trace (expressed as standard deviation) have values of the same order of magnitude (Fig. 3b). The determination of the amplitudes ΔP_i of the different processes presented no problem. However, small values of τ_i close to the time resolution of the instrument or large values of τ_i close to or larger than the measured time interval have large errors.

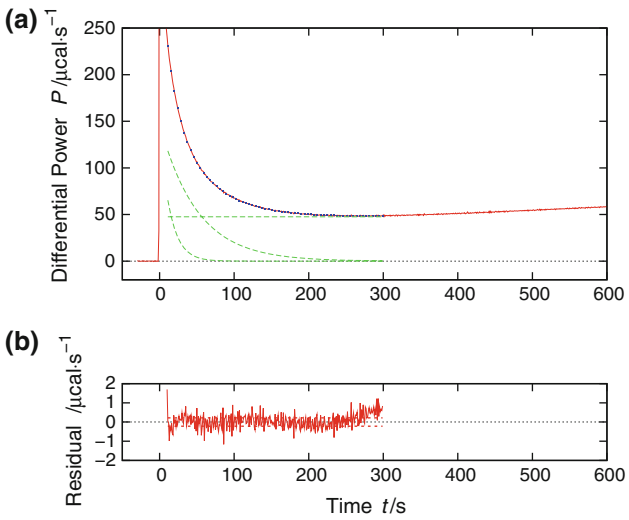

Fig. 3 **a** Deconvolved trace of DMPC at 24.02°C (*red/solid line*), model fit according to Eq. 4 (*filled square symbols*, not all points shown) with amplitudes $\Delta P_{\text{base}} = 47.6$ µcal/s, $\Delta P_1 = 142.9$ µcal/s, $\Delta P_2 = 147.5$ µcal/s and relaxation times $\tau_1 = 14$ s and $\tau_2 = 50$ s; single terms of Eq. 4 are shown as *green dashed lines*. **b** Residuals (*red/solid line*) in comparison with the standard deviation σ_P (*red/dotted line*) as determined from the pretrigger points ($\sigma_P = 0.21$ µcal/s)

For small amplitudes the error for the determined τ_i-values increased also. This occurred regularly at the beginning and the end of the measured temperature interval where small amplitudes are observed.

Results

DSPC

Deconvolved kinetic P–t-traces of DSPC show two relaxation processes that could be resolved (Fig. 4a). Overall, a temperature interval of 1 K was investigated. The amplitude at a time 10 s after the jump is low at the lower end of the studied temperature interval (black line in Fig. 4a). It increases to a maximum value at 54.70°C (green line) and finally decreases again. The blue trace corresponds to a curve measured at the upper end of the temperature range. It is clearly evident that faster processes that are not resolvable because of the limited time resolution of the instrument are also present. The heat-uptake connected with these fast processes corresponds to the area of the peak up to a time of 10 s after the p-jump. The amplitudes ΔP_i as determined by regression analysis are shown in Fig. 4b. It can be seen that the baseline shift ΔP_{base} is much smaller compared with the amplitudes ΔP_i. Values of ΔP_2 belonging to the slower process are smaller by a factor of two compared with ΔP_1, that represents the faster process.

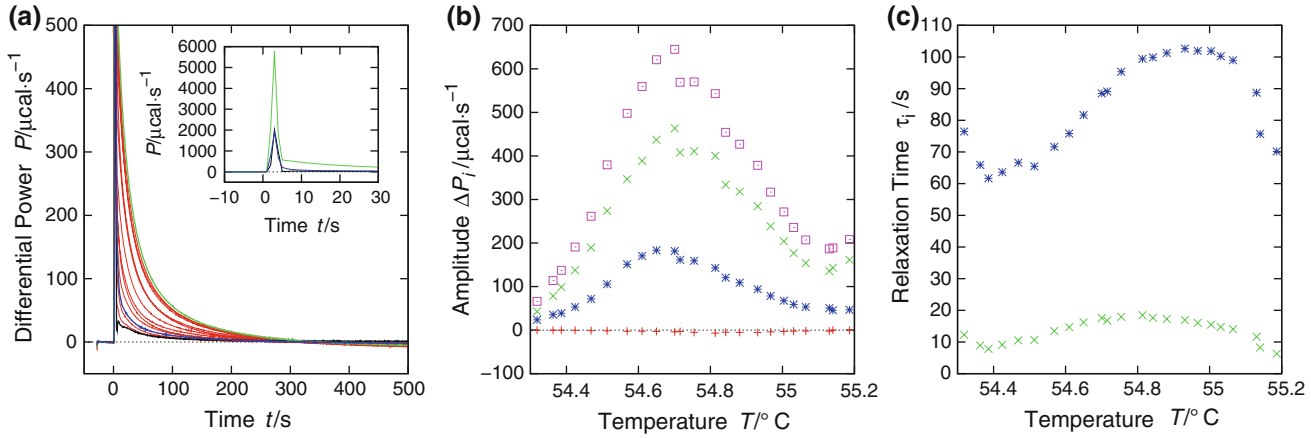

Fig. 4 Transition kinetics of DSPC. **a** Deconvolved PPC heat-flow signals at 52.24°C (*black*), at 54.70°C, the temperature where the maximum amplitude occurs (*green*), at 55.19°C, the highest temperature (*blue*), and at intermediate temperature values (*red*). The *inset* shows a zoomed view of three *curves* to show the total peak height of the traces. **b** Amplitudes ΔP_{base} (*plus signs*), ΔP_1 (*multiplication signs*), ΔP_2 (*asterisks*), and sum of ΔP_i (*open squares*); **c** Relaxation times τ_1 (*multiplication signs*) and τ_2 (*asterisks*)

All curves including the $\sum \Delta P_i$ data show a maximum at 54.70°C. The maximum total amplitude for the two resolved slow processes is a factor of ca. 8 lower than the total experimental amplitude (inset to Fig. 4a). The area under the sharp peak (green curve in inset of Fig. 4a) comprises approximately 50% of the total area. This shows that other faster processes connected with a considerable heat uptake because of the pressure induced transition occur which are not resolvable by the instrument.

The relaxation time constants τ_i are shown in Fig. 4c. Values of τ_1 display a maximum of 18 s at 54.81°C. The maximum of τ_2 has a value of 103 s and is at a slightly higher temperature of 54.93°C. The τ_i versus T curves exhibit a not expected increase of τ_i at the lower end of the monitored temperature range. This is probably an artefact, because of the strong decrease of the amplitude and the concomitant increase in errors in the fitting procedure.

DPPC

The kinetic traces of DPPC suspensions in Fig. 5a are qualitatively similar to those measured for DSPC. The curve with the largest amplitude can be found at 41.65°C (green trace). The amplitude again becomes smaller at lower and higher temperatures. The investigated temperature interval for DPPC is smaller (0.3 K), because of the sharper transition of DPPC compared with DSPC. Amplitude data in the range from 10 to 300 s were used for a regression analysis. The determined amplitudes are shown in Fig. 5b and display maxima centred at 41.67°C (ΔP_1) and 41.60°C (ΔP_2). The $\sum \Delta P_i$-data exhibit a maximum at

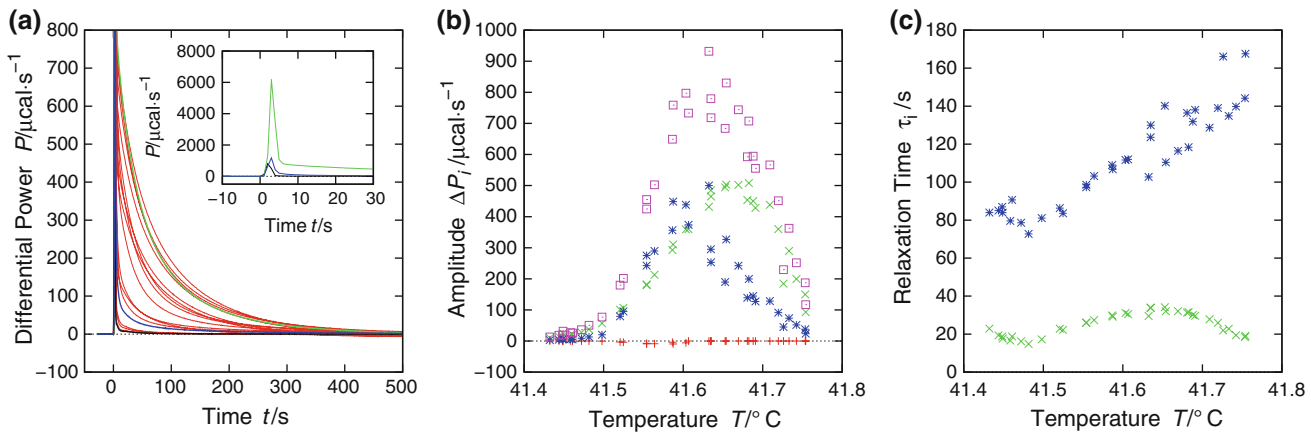

Fig. 5 Transition kinetics of DPPC. **a** Deconvolved PPC heat-flow signals at 41.43°C (*black*), at 41.65°C, the temperature where the maximum amplitude occurs (*green*), at 41.75°C, the highest temperature (*blue*), and at intermediate temperature values (*red*). The inset shows a zoomed view of three *curves* to show the total peak height of the traces. **b** Amplitudes ΔP_{base} (*plus sign*), ΔP_1 (*multiplication signs*), ΔP_2 (*asterisks*), and sum of ΔP_i (*open squares*); **c** Relaxation times τ_1 (*multiplication signs*) and τ_2 (*asterisks*)

41.65°C. The relaxation constants τ_i show, again, a maximum as a function of temperature, as expected (Fig. 5c). The largest value for $\tau_1 = 34$ s was found at 41.65°C. For τ_2 the temperature value for the maximum deviates from the previous one. A maximum of 110 s is indicated at 41.60°C, but the values determined above this temperature are increasing and not decreasing with increasing temperature, as expected. This is again because the noise is strongly enhanced at higher temperature, because of the decrease in amplitude. Furthermore these relaxation constants are so high so that their determination cannot be carried out with sufficient precision when using the time window of 300 s. Use of a longer time interval is not appropriate, because of the similar baseline deviations as already shown for DMPC in Fig. 3.

DMPC

The temperature interval investigated for the main transition of DMPC was only 0.15 K because of the extreme cooperativity of the transition. At temperatures close to T_M the heat uptake induced by a p-jump was very high and exceeded the compensation capabilities of the instrument. These curves (not shown) could not be used for further evaluation. Furthermore, the temperature dependence of the heat capacity led to large shifts in the baseline immediately after the jump at longer times, because of the change in temperature of 10^{-5} K/s, as already described and shown in Fig. 3. The traces that could be used for the analysis are shown in Fig. 6a. The amplitude graph (Fig. 6b) exhibits a gap in the range 24.05–24.12°C caused by the problems described above. It can also be seen that the values of the baseline shift P_{base} are in the same order of magnitude as the partial amplitudes ΔP_i. Because of the lack of useful traces in the temperature range between 24.05°C and 24.12°C, no statements about τ_i maximum values can be made. It can be roughly estimated by interpolation of the data in Fig. 6c by eye, that a maximum value of τ_1 is approximately 20 s in the range 24.05–24.10°C and that for τ_2 the value is larger than 100 s.

DMPA

The cooperativity of the main phase transition of phosphatidic acids is generally lower than for the transition of phosphatidylcholines (Blume and Eibl 1979; Elamrani and Blume 1983). Therefore, the investigated temperature range, 0.83 K, is much broader. The trace measured at 49.90°C shows the largest amplitude of all DMPA traces. The kinetics for DMPA are generally faster than those observed for phosphatidylcholines. The traces display oscillations in the first seconds after the p-jumps. However, these are outside the range used for the regression analysis. The amplitudes ΔP_i and the total amplitude $\sum \Delta P_i$ display a maximum at 49.90°C as shown in Fig. 7b. The relaxation constants displayed in Fig. 7c do not show a temperature dependence with a distinct maximum. Values of τ_1 fluctuate in the range 5–10 s, those of τ_2 in the interval 20–45 s. At low and high temperature τ_2 values could not be determined with sufficient precision because of the low amplitude of the slow process. Therefore they are not shown in Fig. 7c.

DMPE

The kinetic traces of DMPE (Fig. 8a) were measured in a temperature interval of 0.7 K centred at T_M. Deconvolution of the traces shows again that two processes are present, a faster one with the larger amplitude and a slower one with

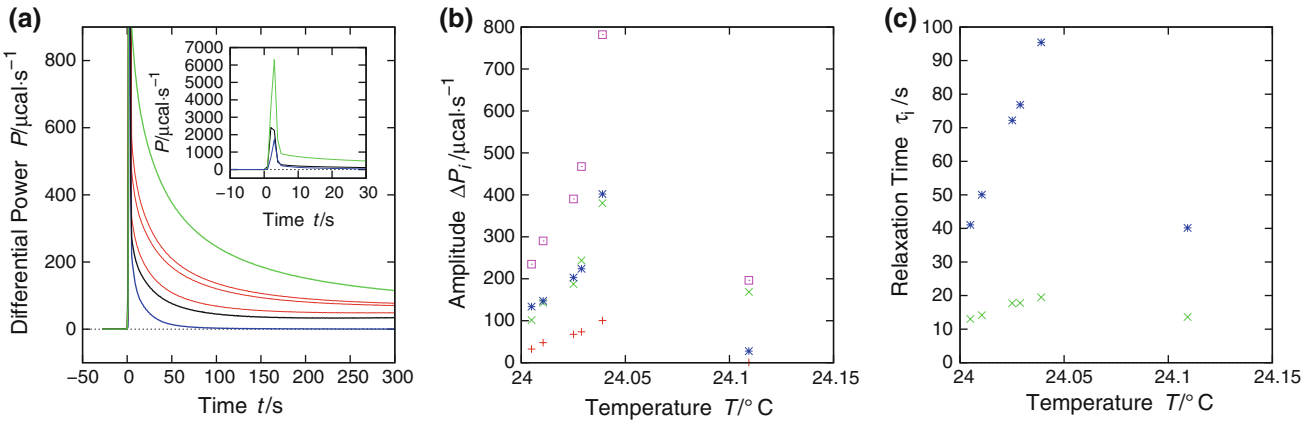

Fig. 6 Transition kinetics of DMPC. **a** Deconvolved PPC heat-flow signals at 24.01°C (*black*), at 24.04°C, the temperature where the maximum amplitude occurs (*green*), at 24.12°C, the highest temperature (*blue*), and at intermediate temperature values (*red*). The *inset* shows a zoomed view of three *curves* to show the total peak height of the traces. **b** Amplitudes ΔP_{base} (*plus signs*), ΔP_1 (*multiplication signs*), ΔP_2 (*asterisks*), and sum of ΔP_i (*open squares*); **c** Relaxation times τ_1 (*multiplication signs*) and τ_2 (*asterisks*)

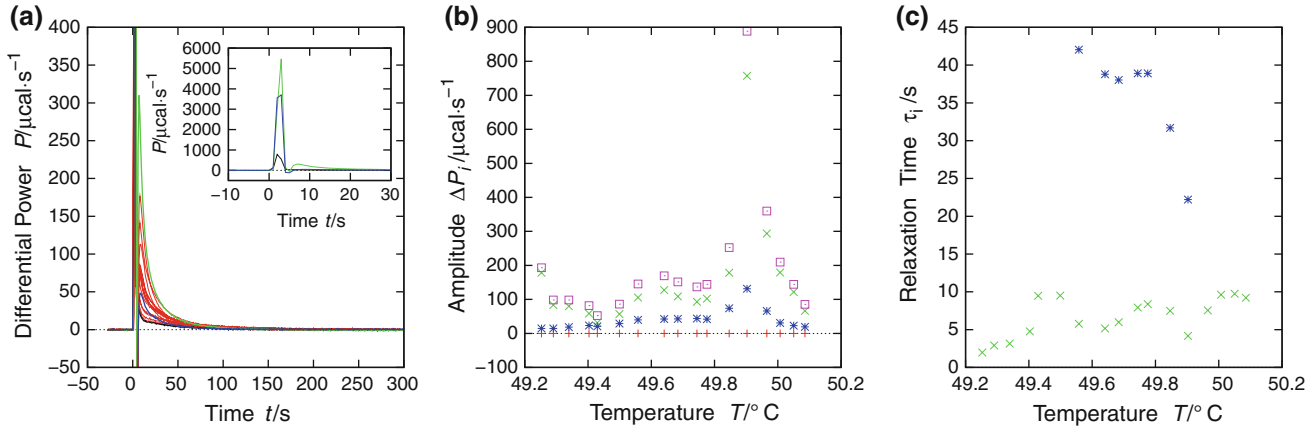

Fig. 7 Transition kinetics of DMPA. **a** Deconvolved PPC heat-flow signals at 49.25°C (*black*), at 49.90°C, the temperature where the maximum amplitude occurs (*green*), at 50.09°C, the highest temperature (*blue*), and at intermediate temperature values (*red*). The *inset* shows a zoomed view of three *curves* to show the total peak height of the traces. **b** Amplitudes ΔP_{base} (*plus signs*), ΔP_1 (*multiplication signs*), ΔP_2 (*asterisks*), and sum of ΔP_i (*open squares*); **c** Relaxation times τ_1 (*multiplication signs*) and τ_2 (*asterisks*). Values for τ_2 below and above the transition midpoint were omitted, because the low amplitude of the slow process led to large errors

smaller amplitude. The amplitude data ΔP_i exhibit a temperature dependence with a maximum of each curve at 50.05°C (Fig. 8a). As mentioned above, the amplitude ΔP_1 comprised more than 80% of the total amplitude. The plot of the temperature dependence of the relaxation time constant τ_1 shows the expected behavior with a maximum at 50.0°C (cf. Fig. 8c). At this temperature, the maximum value of $\tau_1 = 26$ s was found. Determination of the time constant τ_2 was difficult, because of the small corresponding amplitude values of the slow process. τ_2 values in the range of 60–80 s were estimated when the amplitude of the slow process was sufficiently high. At low and high temperatures the amplitude ΔP_2 was so low that the τ_2 values had large errors. They are, therefore, not shown in Fig. 8c.

Discussion

A number of different p-jump investigations on aqueous lipid dispersions, with sometimes contradictory results, have previously been reported. Some of these contradictions are probably because of different observation techniques with different time resolution, for example p-jump with turbidity detection (Gruenewald et al. 1980; Elamrani and Blume 1983; Blume and Hillmann 1986), X-ray scattering (Erbes et al. 2000), FT-IR-spectroscopy (Schiewek and Blume 2009), or calorimetry (Grabitz et al. 2002; Boehm et al. 2007). Other contradictions in results arise because of different underlying concepts of data evaluation.

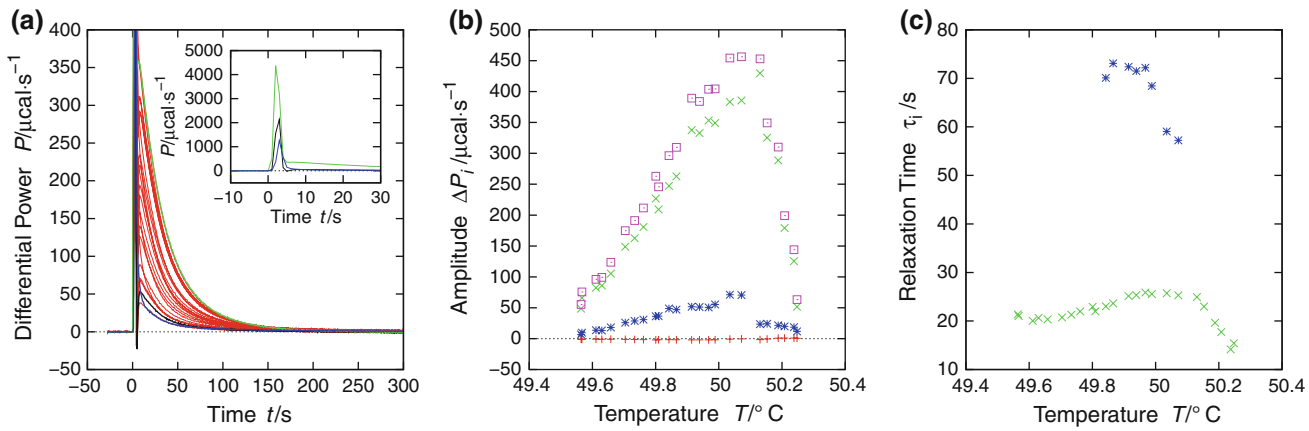

Fig. 8 Transition kinetics of DMPE. **a** Deconvolved PPC heat-flow signals at 49.57°C (*black*), at 50.04°C, the temperature where the maximum amplitude occurs (*green*), at 50.25°C, the highest temperature (*blue*), and at intermediate temperature values (*red*). The *inset* shows a zoomed view of three *curves* to show the total peak height of the traces. **b** Amplitudes ΔP_{base} (*plus signs*), ΔP_1 (*multiplication signs*), ΔP_2 (*asterisks*), and sum of ΔP_i (*open squares*); **c** Relaxation times τ_1 (*multiplication signs*) and τ_2 (*asterisks*).Values for τ_2 below and above the transition midpoint were omitted, because the low amplitude of the slow process led to large errors

The first p-jump relaxation experiment published used turbidity as a detection method (Gruenewald et al. 1980; Elamrani and Blume 1983; Blume and Hillmann 1986). In these measurements on different phospholipids the experiments always showed at least two relaxation processes in the time range of 100 μs–100 ms with maximum values when the jump occurred to the midpoint of the phase transition at ambient pressure. The existence of different relaxation processes was confirmed by T-jump experiments with Joule heating or laser heating using fluorescence probes (Gruenewald 1982; Genz and Holzwarth 1986). Based on these findings a theory was proposed by Eck and Holzwarth (1984), in which the kinetics proceed through several steps covering many orders of magnitude in time constants.

Contradictory results were published when pressure perturbation calorimetry was used. Using this method, relaxation constants up to 45 s for DPPC and 35 s for DMPC were first reported by Grabitz et al. (2002). Similar results were then published by Boehm et al. (2007). The method used for analysis of the PPC data was based on the assumption of a single process. Using this approach the curves could be fitted using the known instrumental response function. As expected, a maximum of the relaxation time was found at the mid-point of the transition. However, in view of the results using other detection methods and particularly our recent results using FT-IR detection (Schiewek and Blume 2009), where we clearly found that processes connected with an increase in the formation of gauche conformers with relaxation times shorter than 20 ms are present, we decided to reinvestigate the transition of lipids using pressure perturbation calorimetry. Our assumption was that fast processes connected with a heat uptake with relaxation times shorter than the instrumental response time should be visible in the PPC experiment when a model-free approach for the data evaluation was used.

Using the MicroCal PPC-add-on, our equipment is similar to the instrument that was used by Boehm et al. Our approach, consisting of the numerical deconvolution of the signal and a fit of a relevant data interval, has the advantage that amplitudes caused by the heat flow due to fast processes are clearly visible. Because kinetic information cannot be obtained for these processes they are not used for further processing. In addition, the use of an incorrect response function will have minimal effects on our results, because this influences only the very first points measured after the jump and these data were not used for fitting.

Our time-resolved pressure perturbation calorimetry data show clearly—just as other p-jump experiments using different detection methods did (Gruenewald et al. 1980; Elamrani and Blume 1983; Schiewek and Blume 2009)—that the main phase transition is a multiprocess transition with time constants having values of different orders of magnitudes. The slower the individual process, the lower is its fraction of the total transition heat uptake. Two processes could be resolved but the deconvolved traces also show faster, not resolvable processes, which is indicated by the large peak that appears at ca. 4 s immediately after the p-jump. At the transition midpoint, where the amplitudes have their highest values, these fast processes are connected with ca. 50% of the total heat uptake. As mentioned above, our previous p-jump experiments with FT-IR detection showed that fluidization of the chains leading to an increase in gauche conformers is, indeed, partly a fast process with relaxation times below 20 ms. As this fluidization of the chains requires an uptake of heat from the surroundings it should also be visible using time-resolved PPC. This is indeed the case.

Values for the relaxation time τ_1 of the faster process for each lipid do not exactly match the data reported in the literature. This may be because of the different analytical approach, as described above. In contrast to Grabitz et al. (2002) and Boehm et al. (2007) we found different values for phosphatidylcholines having a different chain length. Our investigations show also a clear influence of the head group on the transition kinetics. Within the set of lipids having C_{14}-hydrocarbon chains, DMPC exhibits the slowest transition. DMPE, which also has a zwitterionic head group, shows shorter τ_2-values. The shortest τ_2 relaxation time was determined for DMPA. It can be concluded, that the slow processes, which are likely to be connected with water reallocation, become faster for lipids having stronger ionic head group interactions and, therefore, weaker interactions with the water molecules in the inter-lamellar space. However, this does not necessarily mean that the processes not resolvable by PPC also become faster. On the contrary, for the DMPA using turbidity detection the relaxation time was found to increase (Blume and Hillmann 1986).

When comparing molecules having the same headgroups (phosphatidylcholines) but different hydrocarbon chain length one can see that the transition slows down within the series from DSPC over DPPC to DMPC. This shows the effect of cooperativity of the transition, that is much more pronounced for DMPC than for DSPC. Unfortunately, high cooperativity leads to sharp heat capacity profiles and a disturbing heat flow becomes visible because of the temperature change that is non-zero for instrumental reasons. This prevents the determination of the relaxation times for DMPC and partially for DPPC.

The results obtained here are in agreement with those from previous experiments and with published theoretical models showing the multi-step nature of the transition (Kanehisa and Tsong 1978). In the latter model nucleation and domain growing steps are assumed, with nucleation as

the rate-determining step. In a more detailed model proposed by Eck and Holzwarth (1984) the transition proceeds through several steps covering many orders of magnitude in time constants.

A recent publication using molecular modelling based on a coarse-grained model of a lipid bilayer also supports the previous models and our conclusion on the multi-step nature of the transition (Marrink et al. 2005). Marrink et al. found that the critical step in the transition is the formation of a cluster of ca. 20–80 lipids spanning both monolayers. Once the nucleation of clusters of the opposite phase had occurred, fast growth of the clusters was observed. However, growth slowed down again when multiple domains started to interact with each other. Domains of the opposite phase can be entrapped in a network of the initial phase. Finally, "optimization" of the cluster sizes occurred. The transformation was therefore described by four steps, namely nucleation, growth, limited growth, and optimization. At least in the first three steps a change in chain order of the system is occurring, leading to heat uptake for the case of a melting transition. These three steps should be "visible" using turbidity as a method, or FT-IR and PPC. The optimization step observed for a single bilayer in the model calculation might not be visible using techniques that are only sensitive to the properties of individual molecules. It remains unclear whether the observed slow processes connected with the redistribution of water observed using X-ray techniques are connected with heat effects or not and would therefore be visible by time-resolved PPC. This "optimization" step would probably not be visible using FT-IR as a detection method.

Based on the results of the simulation of a phase transition using coarse-grained model for the lipid bilayer, it becomes quite obvious that different detection methods will lead to different results for the time constants for the lipid melting transition. However, it is also clear that this transition is a multi-step process and that several steps in the transition are connected with a change in chain order and, therefore, heat uptake. Our time-resolved PPC experiments support the previous findings and the results of the modelling calculations, because they show that the heat-uptake also is, indeed, a multi-step process.

Acknowledgments We thank Günter Hempel from the Institute of Physics of the Martin-Luther-University Halle-Wittenberg for help and discussion.

References

Blume A, Eibl H (1979) The influence of charge on bilayer membranes. calorimetric investigations of phosphatidic acid bilayers. Biochim Biophys Acta 558:13–21

Blume A, Hillmann M (1986) Dimyristoyl phosphatidic acid cholesterol bilayers thermodynamic properties and kinetics of the phase transition as studied by the pressure jump relaxation technique. Eur Biophys J 13:343–353

Boehm K, Guddorf J, Hinz HJ (2007) Application of pressure modulated differential scanning calorimetry to the determination of relaxation kinetics of multilamellar lipid vesicles. Biophys Chem 126:218–227

Eck V, Holzwarth JF (1984) Fast dynamic phenomena in vesicles of phospholipids during the phase transition. In: Mittal KL, Lindmann B (eds) Surfactants in solution. Plenum Press, New York, pp 2059–2079

Eigen M (1968) Die "unmeßbar" schnellen Reaktionen (Nobel-Vortrag). Angew Chem 80:892–906

Elamrani K, Blume A (1983) Phase-transition kinetics of phosphatidic acid bilayers, a pressure-jump relaxation study. Biochemistry 22:3305–3311

Erbes J, Gabke A, Rapp G, Winter R (2000) Kinetics of phase transformations between lyotropic lipid mesophases of different topology: a time-resolved synchrotron x-ray diffraction study using the pressure-jump relaxation technique. Phys Chem Chem Phys 2:151–162

Genz A, Holzwarth JF (1986) Dynamic fluorescence measurements on the main phase-transition of dipalmitoylphosphatidylcholine vesicles. Eur Biophys J 13:323–330

Grabitz P, Ivanova VP, Heimburg T (2002) Relaxation kinetics of lipid membranes and its relation to the heat capacity. Biophys J 82:299–309

Gruenewald B (1982) On the phase-transition kinetics of phospholipid-bilayers. Relaxation experiments with detection of fluorescence anisotropy. Biochim Biophys Acta 687:71–78

Gruenewald B, Blume A, Watanabe F (1980) Kinetic investigations on the phase-transition of phospholipid-bilayers. Biochim Biophys Acta 597:41–52

Kanehisa MI, Tsong TY (1978) Cluster model of lipid phase transitions with application to passive permeation of molecules and structure relaxations in lipid bilayers. J Am Chem Soc 100:424–432

Kusube M, Matsuki H, Kaneshina S (2005) Thermotropic and barotropic phase transitions of N-methylated dipalmitoylphosphatidylethanolamine bilayers. Biochim Biophys Acta 1668:25–32

Lin LN, Brandts JF, Brandts JM, Plotnikov V (2002) Determination of the volumetric properties of proteins and other solutes using pressure perturbation calorimetry. Anal Biochem 302:144–160

Liu NI, Kay RL (1977) Redetermination of the pressure dependence of the lipid bilayer phase transition. Biochemistry 16:3484–3486

Marrink SJ, Risselada J, Mark AE (2005) Simulation of gel phase formation and melting in lipid bilayers using a coarse grained model. Chem Phys Lipids 135:223–244

Nelder JA, Mead R (1965) A simplex-method for function minimization. Comput J 7:308–313

Plotnikov VV, Brandts JM, Lin LN, Brandts JF (1997) A new ultrasensitive scanning calorimeter. Anal Biochem 250:237–244

Press WH, Flannery BP, Teukolsky SA, Vetterling WT (1989) Numerical recipes—the art of scientific computing. Cambridge University Press, Cambridge

Schiewek M, Blume A (2009) A pressure jump relaxation study of lipid membrane phase transitions using time-resolved FTIR spectroscopy. Eur Biophys J 38:219–228

Schiewek M, Krumova M, Hempel G, Blume A (2007) An apparatus for pressure jump experiments up to 100bar and millisecond resolution using IR-spectroscopy as a detection system. Rev Sci Instrum 78:045101

Winter R, Czeslik C (2000) Pressure effects on the structure of lyotropic lipid mesophases and model biomembrane systems. Z Kristallogr 215:454–474